Electronic Supplementary Material

Docking MOF crystals on graphene support for highly selective electrocatalytic peroxide production

Xiaofeng Huang[1], Peter Oleynikov[1], Hailong He[1], Alvaro Mayoral[1], Linqin Mu[2], Feng Lin[2], and Yue-Biao Zhang[1] (✉)

[1] *School of Physical Science and Technology, ShanghaiTech University, Shanghai 201210, China*
[2] *Department of Chemistry, Virginia Tech, Blacksburg, VA 24061, USA*

Supporting information to https://doi.org/10.1007/s12274-021-3382-3

Section S1 Experimental Procedure

Section S1.1 Materials synthesis

Graphite paper, N,N-dimethylformamide (DMF), N,N-diethylformamide (DEF), Na_2SO_4, KCl, potassium ferricyanide, potassium ferrocyanide, and $Co(NO_3)_2{\cdot}6H_2O$ were purchased from Sinopharm Chemical Reagent Co. Ltd., tetracarboxyphenyl porphyrin (TCPP), ferrocene were purchased from Tokyo Chemical Industry Co. Ltd. Graphene oxide (GO) was purchased from commercial source. These reagents were used as received without any further treatment. Milli-Q water with a conductivity of 18.2 MΩ cm is used throughout the experiment.

EG: Few-layer graphene is synthesized through electrochemical exfoliation in two-electrode configuration with slight modification to previous reports [S1] as described in the manuscript. Briefly, graphite paper is cut into slides an area of 1.0 × 3.0 cm^2 and used as the working electrode without any further pretreatment while platinum wire was used as the counter electrode. The electrochemical exfoliation was conducted in 0.1 M Na_2SO_4 with +10 V bias applied to the graphite paper. During this process, huge amount of gas was evolved from both electrodes and black curling substances are released from graphite paper. After completion, black sediments and suspended substances were collected through vacuum filtration, washed with copious amount of ultrapure water, and finally dried under air. The as-synthesized sample was denoted as EG. A stock solution of 2 mg mL^{-1} of EG in DMF solution is also prepared for synthetic purposes.

NG: NG was synthesized by facilely refluxing in DMF under inert gas. Typically, 10 mg EG was dispersed in 20 mL DMF solution by ultrasonication for 15 min. A black homogeneous solution was formed and then heated at certain temperature to reflux for a certain time span under N_2 protection. After completion, the mixture was dried under vacuum. The as-synthesized sample was denoted as NG.

NG': NG' is prepared through a similar procedure to NG except that a high-power ultrasonic probe (20 kHz, 120 W, Fisher Scientific) was used to sonicate and fully disperse EG in DMF.

MOF: MOF was synthesized by a facile solvothermal strategy with slight modification to the literature[S2]. In a typical synthesis, TCPP (23.7 mg, 0.03 mmol) was dissolved in 6 mL DEF and ethanol mixed solution (V_{DEF}:V_{EtOH} = 3:1). After sonication for 15 min, $Co(NO_3)_2{\cdot}6H_2O$ (26.2 mg, 0.09 mmol) was then added and again sonication for further 15 min. The mixture was transferred to a 10 mL Teflon-lined stainless-steel autoclave and kept at 80 °C for 72 h. After cooling down to room temperature at a ramping rate of 0.05 °C min^{-1}, the dark red solids were collected by vacuum filtration and washed by ethanol three times. The product was dried under vacuum and denoted as MOF.

MOF@NG: MOF@NG was synthesized as follows. EG (10 mg) and TCPP (23.7 mg, 0.03 mmol) was dispersed in 20 mL DMF under intense sonication (53 kHz, 100 W, Shanghai Kudos ultrasonic cleaner) to form a homogeneous solution. It was then heated under reflux for 20 h under N_2 protection. Post-refluxed mixtures were vacuum dried and re-dissolved in 6 mL DEF and ethanol mixed solution (V_{DEF}:V_{EtOH} = 3:1). After sonication for 15 min, $Co(NO_3)_2{\cdot}6H_2O$ (26.2 mg, 0.09 mmol) was then added and again sonication for another 15 min. The mixture was transferred to a 10 mL Teflon-lined stainless-steel autoclave and kept at 80 °C for 72 h. After cooling down to room temperature at a ramping rate of 0.05 °C min^{-1}, the precipitates were collected and washed by ethanol for three times. The product was dried under vacuum and denoted as MOF@NG.

MOF@EG: MOF@EG control sample was synthesized as follows. EG (10 mg) and TCPP (23.7 mg, 0.03 mmol) was dispersed in 6 mL DEF and ethanol mixed solution (V_{DEF}:V_{EtOH} = 3:1) under sonication. $Co(NO_3)_2{\cdot}6H_2O$ (26.2 mg, 0.09 mmol) was subsequently added and the mixture was further sonicated for another 15 min. The resulting mixture was transferred to a 10 mL Teflon-lined stainless-steel autoclave and kept at 80 °C for 72 h. After cooling down to room temperature at a ramping rate of 0.05 °C min^{-1}, the precipitates were collected and washed by ethanol for three times. The product was dried under vacuum and denoted as MOF@EG.

MOF@GO: The synthesis of MOF@GO is similar to MOF@NG with the exception that GO is used.

CoTCPP@NG: CoTCPP is synthesized according to literature.[S3] The synthesis of CoTCPP@NG is similar to that of MOF@NG except that CoTCPP is used and no Co(NO3)2·6H2O is added. Products are collected and dried under vacuum.

Address correspondence to zhangyb@shanghaitech.edu.cn

Section S1.2 Electrochemical Tests

For modification of the working electrode (glassy carbon disk), 10 mg of the catalyst is dispersed in 1 mL ethanol containing 10 μL 5% Nafion-117 solution (Dupont) to form a catalyst ink. After being thoroughly sonicated for 15 min, 10 μL catalyst ink is drop casted onto RRDE and dried under gentle N_2 flow. Before electrochemical testing, Pt ring is activated in 0.5 M H_2SO_4 by conducting cyclic voltammetry in the potential range between -0.3 V and +1.2 V (vs. SCE) for 20 cycles at a scan rate of 50 mV s^{-1}. The collection efficiency is determined to be 0.33 in ferricyanide/ferrocyanide solution, which is quite close to the value (0.37) provided by the manufacturer. Prior to acquiring the polarization curve, ultrapure (99.999%) N_2/O_2 is purged into the electrolyte solution for at least 15 min to fully expel impurity gases. During RRDE measurements, the Pt ring potential is set at +1.2 V (vs. SCE). Constant potential electrolysis of O_2 is conducted in a home-made H-type electrochemical cell. The cathodic and anodic compartment is separated by Nafion-117 membrane (Dupont).

Determining the ECSA the catalysts. The electrochemically active surface area (ECSA), was determined using cyclic voltammogram in MeCN solution containing 0.1 M tetra(n-butyl)ammonium hexafluorophosphate as supporting electrolyte and 5 mM ferrocene as probe molecule. The electrochemical setup and catalyst modification are identical to those described in the experimental section. ECSA is calculated through the Randles-Sevcik equation as follows,

$$i_p = 2.69\times10^5 n^{3/2} A D^{1/2} C v^{1/2} \quad (1)$$

Where i_p is the peak current, n the electron transferred (n = 1 for ferrocene), A the ECSA, D the diffusion constant of ferrocene in MeCN, C the concentration of ferrocene (5 mM), and v the scan rate.

Determining the O_2 adsorption amount. Chronocoulometry is conducted in N_2/O_2 purged 0.5 M H_2SO4 with potential stepping from 0.6 V to 0.0 V (vs. Ag/AgCl) with a various pulse width. The accumulated charge ΔQ is calculated by subtracting the intercept obtained by the extrapolation from the linear-fitting curve recorded in O_2 from that in N_2. The electrochemical setup and catalyst modification are identical to that described in the experimental section. The O_2 adsorption amount of is thus calculated by the following equation,

$$\Gamma_m(O_2) = \frac{\Delta Q}{nF}\frac{1}{M_{Co}\cdot S_{GC}} \quad (2)$$

in which ΔQ is the net charge accumulated, n the number of electrons from calculated from the following, F the Faraday constant (96485 C mol^{-1}). M_{Co} the value in Table 1 and S_{GC} the area of glassy carbon electrode (0.0707 cm^2).

Determining the number of electrons transferred and hydrogen peroxide yield. The number of electrons per O_2 is calculated using the following equation

$$n = 4\frac{I_d}{I_d + \frac{I_r}{N}} \quad (3)$$

and the peroxide yield is calculated using the following equation

$$Y(H_2O_2) = 200\frac{\frac{I_r}{N}}{I_d + \frac{I_r}{N}} \quad (4)$$

Where Id and Ir is the absolute disk current and ring current at 1600 rpm, respectively. N is the collection efficiency (N = 0.33, determined in $[Fe(CN)_6]^{3-}/[Fe(CN)_6]^{4-}$). Results for Koutecky-Levich (K-L) equation showed much deviation from the results using the above equation (3), as shown in the following Table.

Table. Difference between the number of electrons transferred per O_2 (n) calculated from K-L equation (K-L) of or equation (3) (RRDE). The disk current data are chosen at 0.1 V (vs. RHE) for calculation.

	n		**Difference**
	K-L	RRDE	***n***(RRDE)-***n***(KL)
NG	2.46	3.43	0.97
MOF	1.84	3.61	1.77
MOF|NG	1.99	2.80	0.89
MOF@NG	2.33	2.80	0.47
MOF@EG	2.16	2.88	0.72
MOF@GO	2.98	2.39	-0.59
MOF@NG'	3.25	2.24	-1.01
CoTCPP@NG	2.51	2.88	0.37

The difference of number of electrons transferred per O_2 is very large between the two calculation methods. Reference by Swager et al.[S4] recommended that the utilization of K-L equation to calculate the number of electrons transferred per O_2 due to the convectional factors. However, according to our constant potential electrolysis experiment (at 0.4 V vs. RHE), the produced H_2O_2 concentration are in good agreement with the n calculated by equation 3. Therefore, we adopt equation (3) to calculate n.

Section 2 Supporting Experimental Results

Table S1 Fractional atomic coordinates for crystal structure model of MOF.

MOF				
Formula: $C_{576}H_{384}O_{120}N_{48}Co_{36}$				
Crystal system: Tetragonal				
Space group: $P4_2/nmc$(No. 137)				
a = 16.6526 Å; c = 117.4977 Å				
$\alpha = \beta = \gamma = 90°$				
d = 0.6125 g cm^{-3}				
V = 32583.18 Å^3				
Atom	x	y	z	Occupancy
O1	0.17251	0.67206	-0.55098	1
O2	0.17206	0.67251	-0.53236	1
C3	0.05086	0.54936	-0.55194	1
H4	0.07277	0.57159	-0.56002	1
C5	-0.00838	0.48915	-0.55194	1
H6	-0.03070	0.46636	-0.55996	1
C7	0.04936	0.55086	-0.53138	1
H8	0.07159	0.57277	-0.52332	1
C9	-0.01085	0.49162	-0.53140	1
H10	-0.03364	0.46930	-0.52338	1
C11	0.14430	0.64492	-0.54166	1
C12	0.08036	0.58150	-0.54166	1
C13	-0.04166	0.46151	-0.54166	1
C14	-0.10641	0.39874	-0.54166	1
C15	-0.18344	0.42086	-0.54166	1
C16	-0.21047	0.50405	-0.54166	1
H17	-0.17447	0.55817	-0.54166	1
C18	-0.07914	0.31656	-0.54166	1
C19	0.00405	0.28953	-0.54166	1
H20	0.05817	0.32553	-0.54166	1
O21	-0.32794	0.67251	0.28236	1
O22	-0.32794	0.67251	0.30098	1
C23	-0.45064	0.55086	0.28138	1
H24	-0.42841	0.57277	0.27332	1
C25	-0.51085	0.49162	0.28140	1
H26	-0.53364	0.46930	0.27338	1
C27	-0.45064	0.55086	0.30194	1
H28	-0.42841	0.57277	0.31002	1
C29	-0.51085	0.49162	0.30194	1
H30	-0.53364	0.46930	0.30996	1
C31	-0.35570	0.64492	0.29166	1
C32	-0.41964	0.58150	0.29166	1
C33	-0.54166	0.46151	0.29166	1
C34	-0.60641	0.39874	0.29166	1

C35	-0.68344	0.42086	0.29166	1
C36	-0.71047	0.50405	0.29166	1
H37	-0.67447	0.55817	0.29166	1
C38	-0.57914	0.31656	0.29166	1
C39	-0.49595	0.28953	0.29166	1
H40	-0.44183	0.32553	0.29166	1
O41	-0.82794	0.17251	0.36568	1
O42	-0.82794	0.17251	0.38432	1
C43	-0.95064	0.05086	0.36472	1
H44	-0.92841	0.07277	0.35664	1
C45	-1.01085	-0.00838	0.36474	1
H46	-1.03364	-0.03070	0.35670	1
C47	-0.95064	0.05086	0.38528	1
H48	-0.92841	0.07277	0.39336	1
C49	-1.01085	-0.00838	0.38528	1
H50	-1.03364	-0.03070	0.39330	1
C51	-0.85570	0.14492	0.37500	1
C52	-0.91964	0.08150	0.37500	1
C53	-1.04166	-0.03849	0.37500	1
C54	-1.10641	-0.10126	0.37500	1
C55	-1.18344	-0.07914	0.37500	1
C56	-1.21047	0.00405	0.37500	1
H57	-1.17447	0.05817	0.37500	1
C58	-1.07914	-0.18344	0.37500	1
C59	-0.99595	-0.21047	0.37500	1
H60	-0.94183	-0.17447	0.37500	1
Co61	-0.25000	0.25000	-0.54166	1
Co62	0.25000	-0.25000	-0.55102	1
Co63	0.25000	-0.25000	-0.53230	1
O64	0.25000	-0.25000	-0.56678	1
O65	0.25000	-0.25000	-0.51654	1
H66	0.19448	-0.25000	-0.51352	1
H67	0.30552	-0.25000	-0.56980	1
H68	-0.30552	-0.25000	0.31982	1
H69	-0.19448	-0.25000	0.26352	1
N70	-1.13183	-0.25000	0.37500	1
N71	-0.25000	0.36817	-0.54166	1
H72	-0.25000	-0.19448	0.31982	1
H73	-0.25000	-0.30552	0.26352	1
N74	-0.13183	0.25000	-0.54166	1
N75	-0.63183	0.25000	0.29166	1
H76	-0.69448	0.25000	0.34686	1
H77	-0.80552	0.25000	0.40314	1
H78	0.25000	-0.19448	-0.51352	1
H79	0.25000	-0.30552	-0.56980	1

Co80	-0.25000	-0.25000	0.28230	1
Co81	-0.25000	-0.25000	0.30102	1
O82	-0.25000	-0.25000	0.26654	1
O83	-0.25000	-0.25000	0.31678	1
Co84	-0.75000	0.25000	0.29166	1
Co85	-0.75000	0.25000	0.38436	1
Co86	-0.75000	0.25000	0.36564	1
O87	-0.75000	0.25000	0.34988	1
O88	-0.75000	0.25000	0.40012	1
N89	-0.75000	0.36817	0.29166	1
H90	-0.75000	0.19448	0.34686	1
H91	-0.75000	0.30552	0.40314	1
N92	-1.25000	-0.13183	0.37500	1
Co93	-1.25000	0.25000	0.37500	1

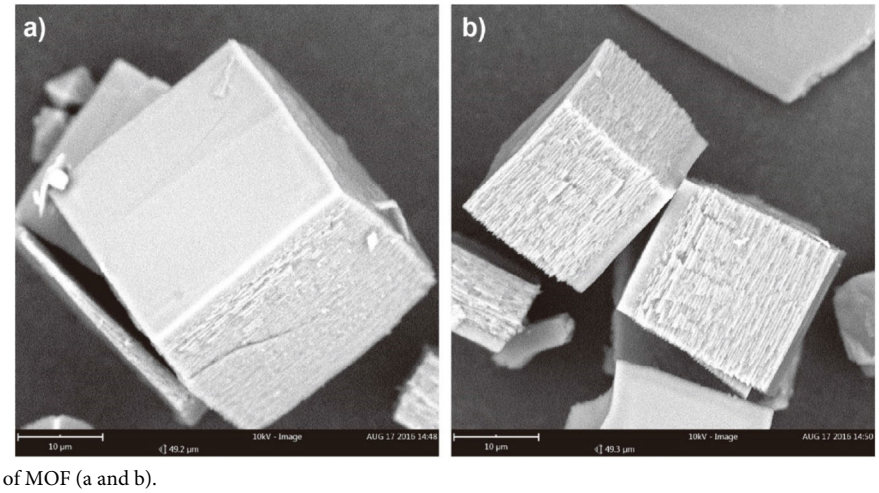

Figure S1 SEM images of MOF (a and b).

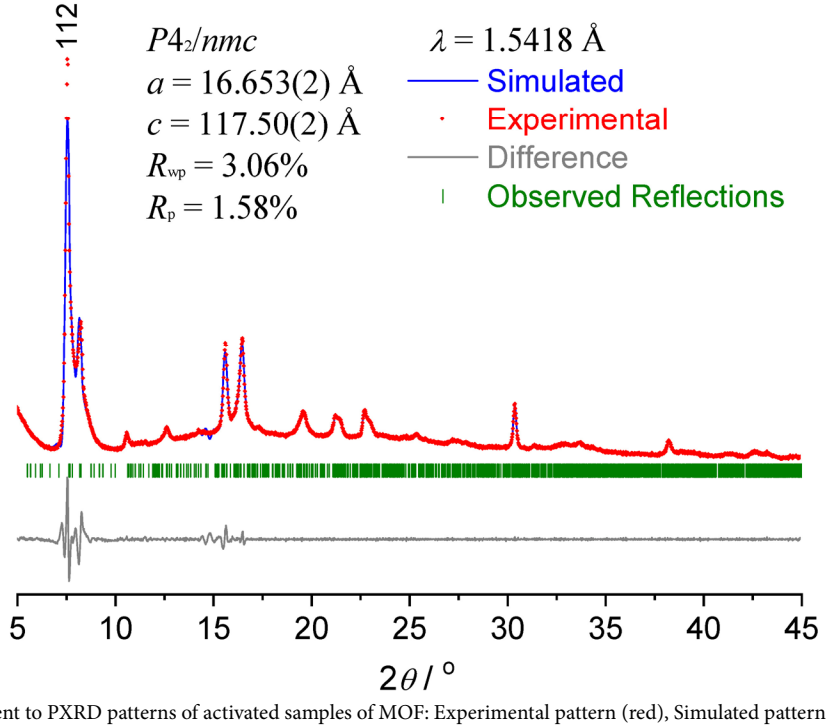

Figure S2 Pawley refinement to PXRD patterns of activated samples of MOF: Experimental pattern (red), Simulated pattern (blue), their difference (gray) and Bragg reflections (green).

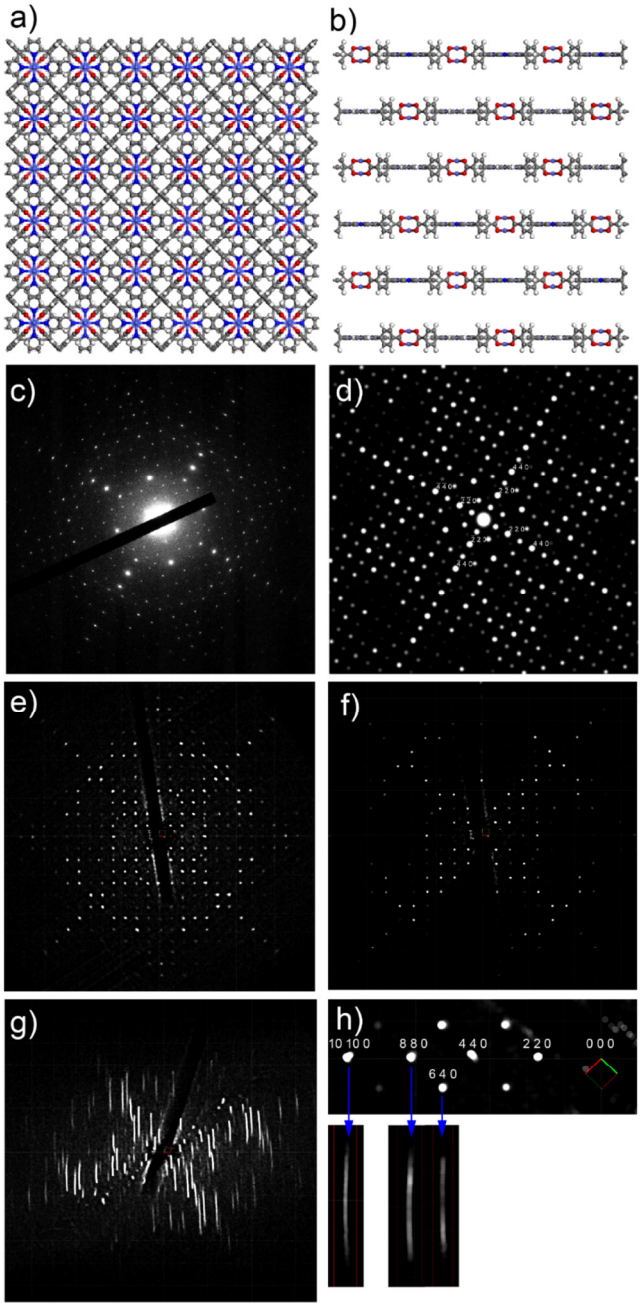

Figure S3 Schematic modelling of MOF viewed from *c* axis (a) and *b* axis (b). Gray, red, blue and violet balls represent carbon, oxygen, nitrogen and cobalt atom, respectively. The experimental SAED pattern of MOF is shown in c) while the simulated pattern (via *SingleCrystal* software) in d); e) shows the whole three-dimensional reconstructed electron diffraction projection and the *hk0* plane cut from the reconstruction; g) Side view of the reciprocal space. The diffusive pattern in g) and the non-uniform intensity modulation in reciprocal rod along *c* axis h) indicates the packing in the *c* direction are disordered.

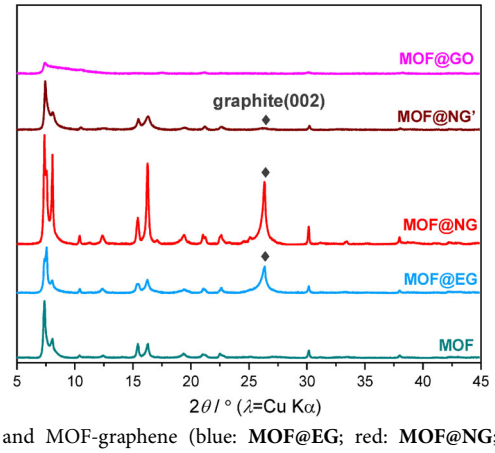

Figure S4 PXRD patterns of **MOF** (cyan) and MOF-graphene (blue: **MOF@EG**; red: **MOF@NG**; dark red: **MOF@NG'**; magenta: **MOF@GO**) nanocomposites.

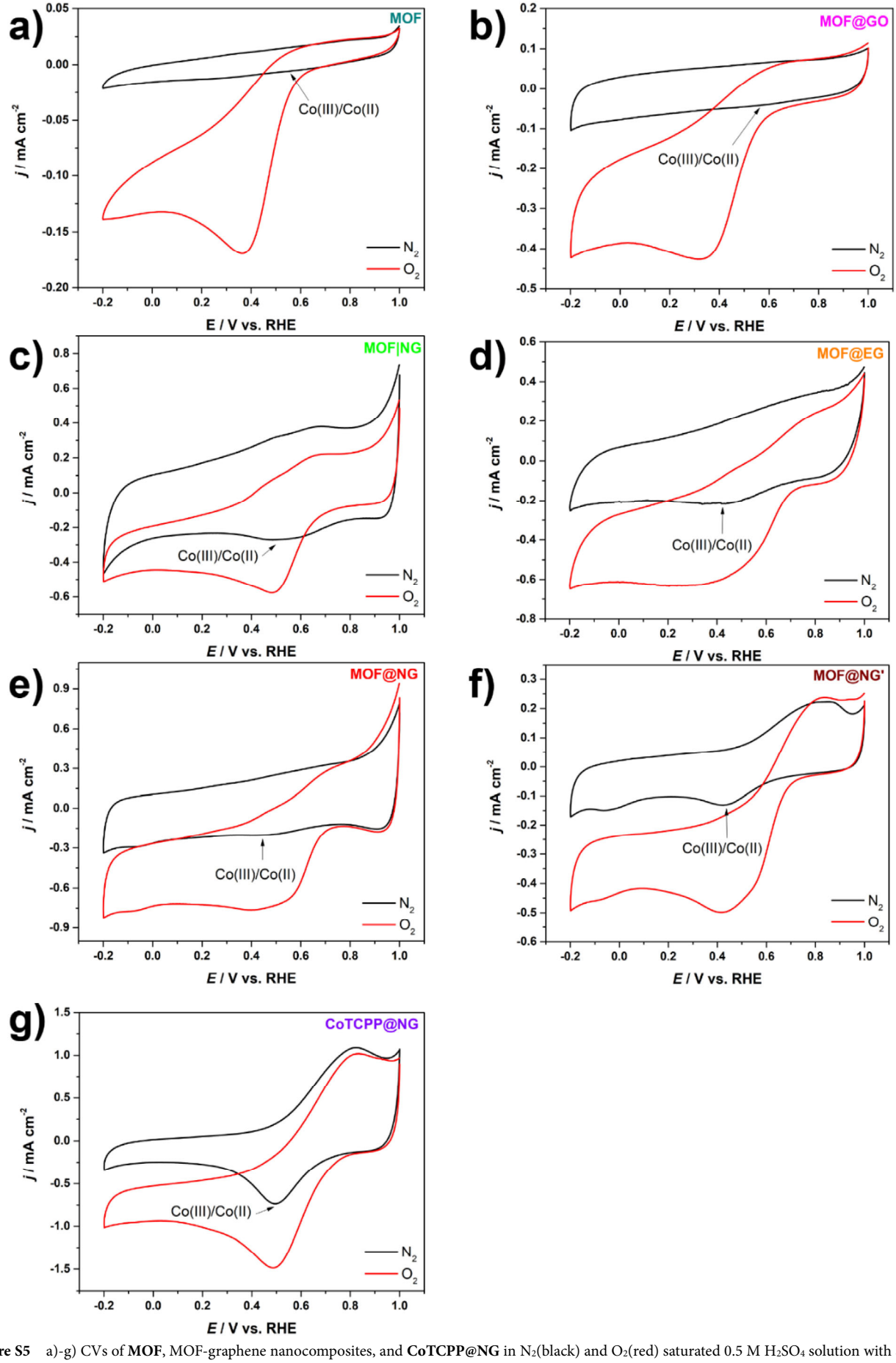

Figure S5 a)-g) CVs of **MOF**, MOF-graphene nanocomposites, and **CoTCPP@NG** in N_2(black) and O_2(red) saturated 0.5 M H_2SO_4 solution with a scan rate of 10 mV s^{-1}.

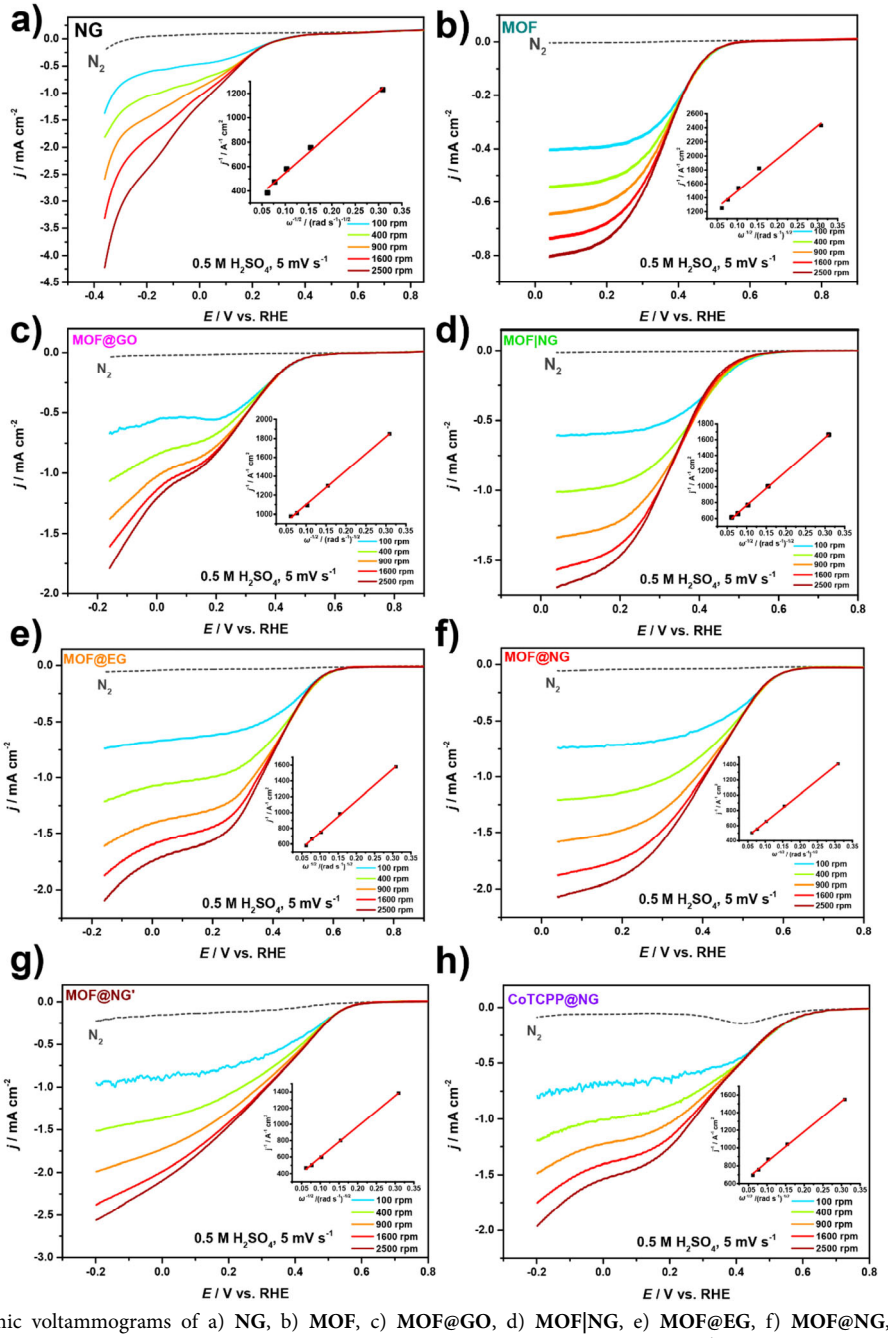

Figure S6 Hydrodynamic voltammograms of a) **NG**, b) **MOF**, c) **MOF@GO**, d) **MOF|NG**, e) **MOF@EG**, f) **MOF@NG**, g) **MOF@NG'** and h) **CoTCPP@NG** in N_2(dash gray line)/O_2(solid colored line) purged 0.5 M H_2SO_4 with a scan rate of 5 mV s^{-1} at the rotation speed of 100, 400, 900, 1600, and 2500 rpm. Inset: Corresponding Koutecky-Levich fitting. These data are not used the calculation of electron numbers.

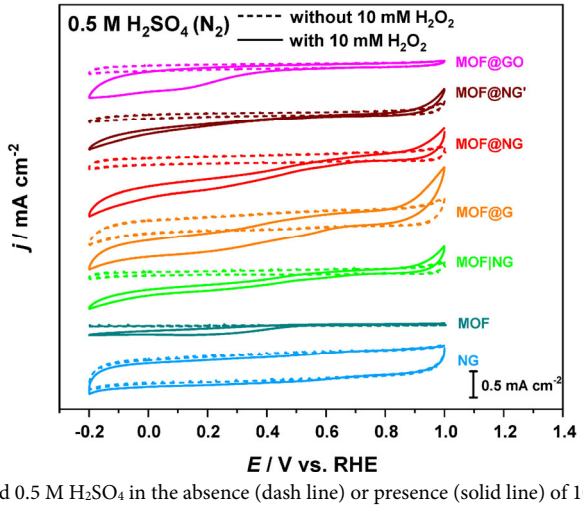

Figure S7 CVs of all samples in N_2 purged 0.5 M H_2SO_4 in the absence (dash line) or presence (solid line) of 10 mM H_2O_2 at a scan rate of 10 mV s^{-1}.

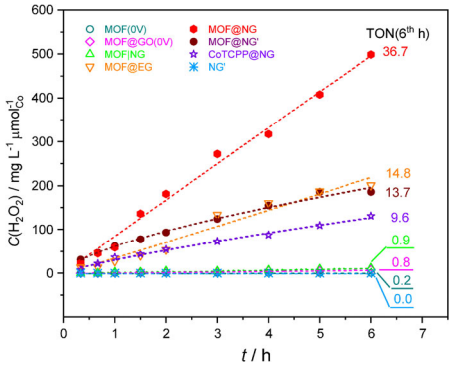

Figure S8 Time-dependence for electro-catalyzed H_2O_2 production in O_2 saturated 0.5 M H_2SO_4 at an applied potential of 0.4 V vs. RHE for 6 h. (0 V for **MOF** and **MOF@GO**). TONs for all electrocatalysts at 6th h are also calculated and displayed.

Table S2 R_{ct} and ECSA of **EG**, **NG**, **GO** and **NG'**.

	[a]ECSA [cm^2]	[b]R_{ct} [Ω]	$\Gamma_m(O_2)$ [g g$^{-1}_C$]
NG	0.272	96.8	1.980×10^{-4}
EG	0.243	105.5	4.526×10^{-5}
NG'	0.135	153.9	5.460×10^{-5}
GO	0.059	297.5	1.262×10^{-4}

[a,b] The determination of ECSA and R_{ct} are identical to that described in Section S1.3.

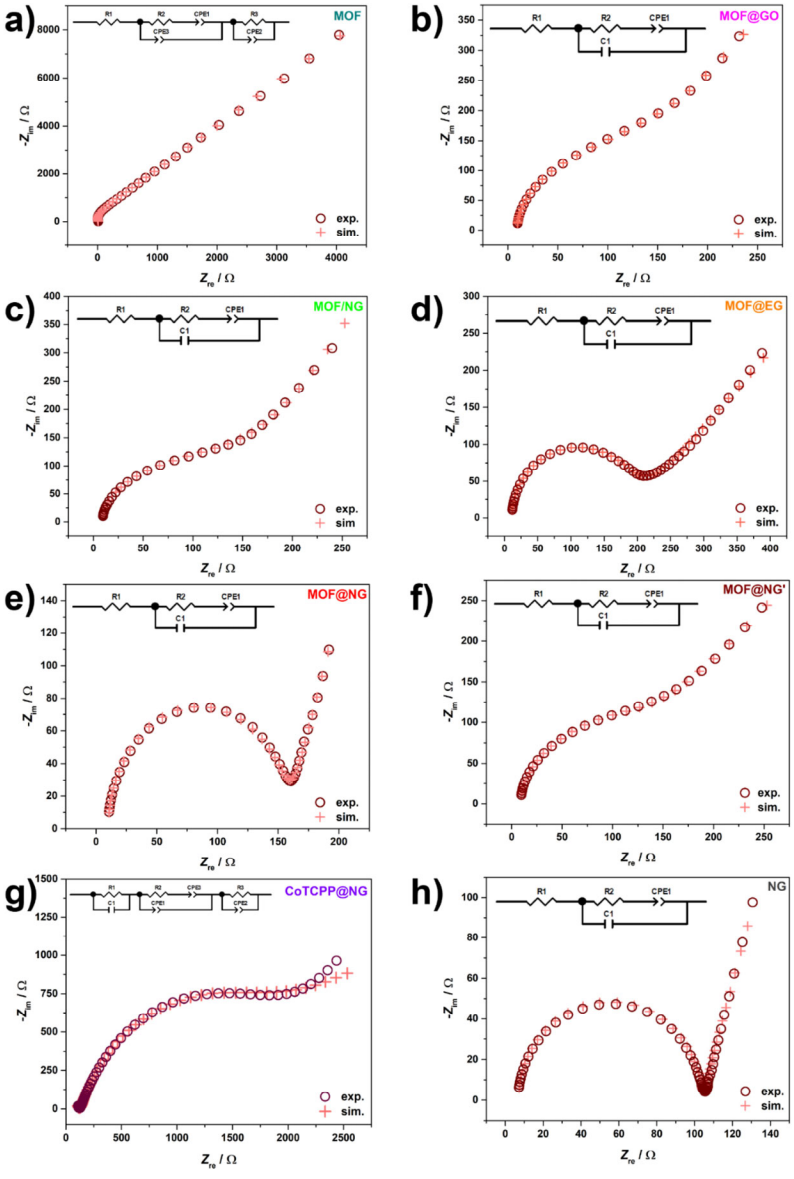

Figure S9 a)-h) Nyquist plot and corresponding fitted equivalent circuit of **MOF**, MOF-graphene derivatives and **CoTCPP@NG**.

Table S3 ORR performance of all samples.

Catalyst	[a]R_{ct} [Ω]	[b]E_{onset} [V vs. RHE]	[c]j_{lim} [mA cm^{-2}]	[d]M_{Co} [μg cm^{-2}]	[e]$MA_{Co}(MA_{cat})$ [mA mg^{-1}]
MOF@NG	148.6	0.57	1.812	6.5	279.6(4.48)
MOF@NG'	174.5	0.50	0.816	9.5	85.9(2.02)
MOF@EG	180.9	0.55	1.504	11.0	136.7(3.72)
MOF|NG	210.2	0.47	1.525	12.2	125.0(3.77)
MOF@GO	286.3	0.46	0.983	10.9	90.2(2.43)
MOF	479.2	0.47	0.732	12.2	60.0(1.81)
CoTCPP@NG	1822	0.57	1.327	13.5	98.3(3.28)

[a]Charge transfer resistance, measured in 0.1 M tetra(n-butyl)ammonium hexafluorophosphate in MeCN containing 5 mM ferrocene in the frequency range from 1-10^6 with an amplitude of 5 mV. The charge transferred resistance is calculated by the fitting of the Nyquist plot using the *ZView* software.

[b,c]Data are collected from rotating-ring disk voltammograms at 1600 rpm. The current density is normalized by the geometric area (0.2475 cm^2) of glassy carbon electrode.

[d]Results are calculated from the results of ICP-OES.

[e]MA_{Co}/MA_{cat}=Mass activity, calculated by normalizing j_{lim} by M_{Co} or the loading amount of catalyst, 0.404 mg cm^{-2}.

Table S4 ORR performance in relation with the concentration of NG.

[a]NG concentration / mg mL^{-1}	E_{onset} / Vvs. RHE	j_p / mA cm^{-2}	[b]ECSA / cm^2	[c]R_{ct} / Ω
0.0	0.55	0.153	0.0429	479.2
0.1	0.61	0.164	0.0366	252.2
0.3	0.62	0.182	0.0531	194.6
0.5	0.66	0.229	0.0562	182.1
0.75	0.66	0.364	0.0715	160.9
1	0.66	0.569	0.0949	158.2
1.25	0.67	0.455	0.126	162.5
1.5	0.69	0.627	0.122	148.6
2.0	0.68	0.559	0.125	149.4
2.5	0.68	0.876	0.121	148.7

[a] Initially added amount of **NG**

[b,c] The determination of ECSA and R_{ct} are identical to that described in Section S1.3.

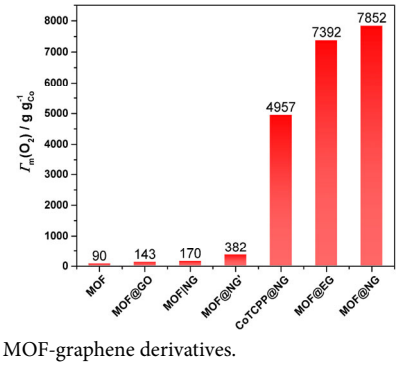

Figure S10 Amount of O_2 adsorption on **MOF** and MOF-graphene derivatives.

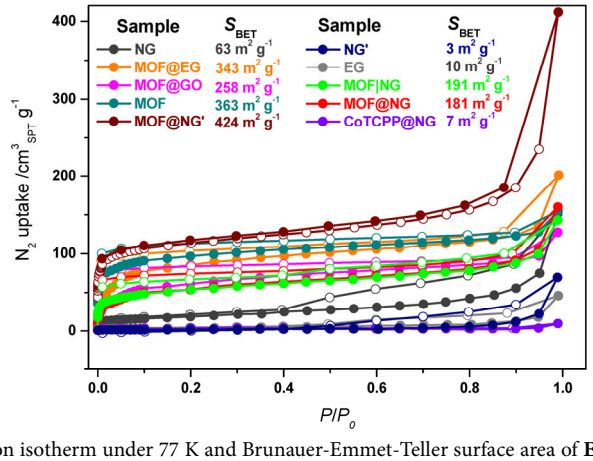

Figure S11 N_2 adsorption and desorption isotherm under 77 K and Brunauer-Emmet-Teller surface area of **EG**, **NG**, **NG'**, **CoTCPP@NG**, **MOF** and all other MOF-graphene nanocomposites.

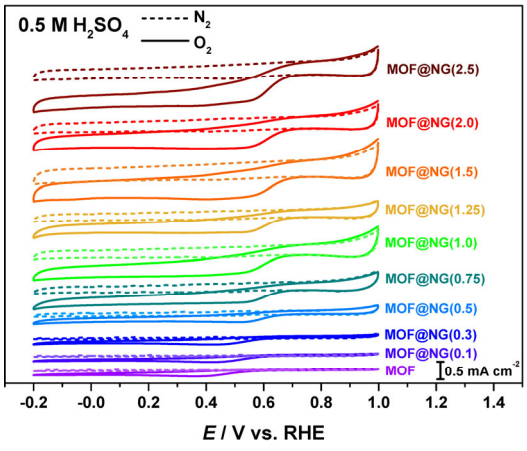

Figure S12 CVs of MOF in compositing with different concentrations of **NG** in N_2(dotted line)/O_2(solid line) purged 0.5 M H_2SO_4 with a scan rate of 10 mV s^{-1}.

Table S5 ORR performance in comparison with references.

Catalyst	M_{Co} or $M_{cat.}$	MA [mA mg^{-1}_{M}]	Electrolyte(scan rate)	Ref.
MOF@NG	6.5 μg cm^{-2}_{Co}	279.6		
MOF@NG'	9.5 μg cm^{-2}_{Co}	85.9	0.5 M H_2SO_4 (5 mV s^{-1})	This work
Pt/C(20%)	80.8 μg cm^{-2}_{Pt}	52.8		
MWCNT-Co porphyrin	(-)	(-)	1.0 M $HClO_4$	[S4]
Pt-Pd nanodendrites	15.3 μg cm^{-2}_{Pt}	204	0.1 M $HClO_4$ (10 mV s^{-1})	[S5]
Pd@Pt_{nL}(n>1)	30.6 μg cm^{-2}_{Pt}	230	0.1 M $HClO_4$ (10 mV s^{-1})	[S6]
Pt_3Co-400	17.7 μg cm^{-2}_{Pt}	160	0.1 M $HClO_4$ (10 mV s^{-1})	[S7]
AgPd@Pt/C	15.0 μg cm^{-2}_{Pt}	220	0.1 M $HClO_4$ (20 mV s^{-1})	[S8]
MWCNT-CoP	155 μg $cm^{-2}_{cat.}$	(-)	0.5 M H_2SO_4 (5 mV s^{-1})	[S9]
Fe(DFTPP)-CNTs	1.0 mg $cm^{-2}_{cat.}$	(-)	0.1 M $HClO_4$ (10 mV s^{-1})	[S10]
Co(TMPP)-SWCNT	3.84 mg $cm^{-2}_{cat.}$	(-)	0.1 M H_2SO_4	[S11]
Co-TPFC/MWNT	(-)	(-)	0.5 M H_2SO_4 (10 mV s^{-1})	[S12]
CoTAPP-graphene	1.0 mg $cm^{-2}_{cat.}$	(-)	0.5 M H_2SO_4 (20 mV s^{-1})	[S13]
$(G\text{-dye-FeP})_n$ MOF	185.2 μg $cm^{-2}_{cat.}$	(-)	0.1 M KOH (10 mV s^{-1})	[S14]
$rGO/(Co\text{-}THPP)_7$	(-)	(-)	0.1 M KOH (10 mV s^{-1})	[S15]
CoEtP-DWCNTs	185.2 μg $cm^{-2}_{cat.}$	(-)	0.1 M NaOH (5 mV s^{-1})	[S16]

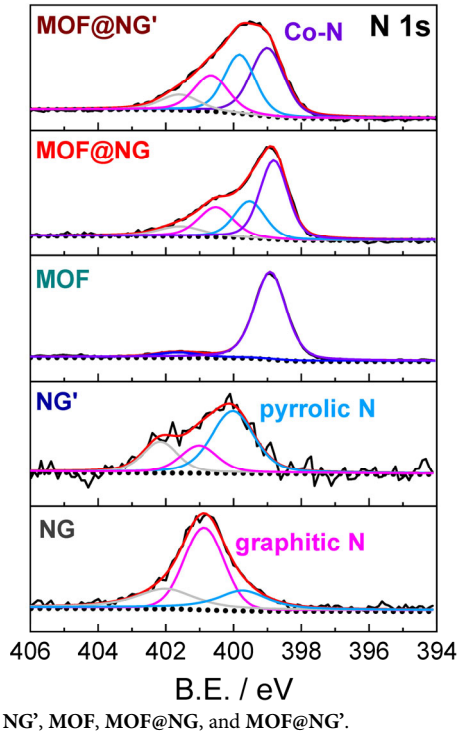

Figure S13 High resolution N *1s* spectra of **NG**, **NG'**, **MOF**, **MOF@NG**, and **MOF@NG'**.

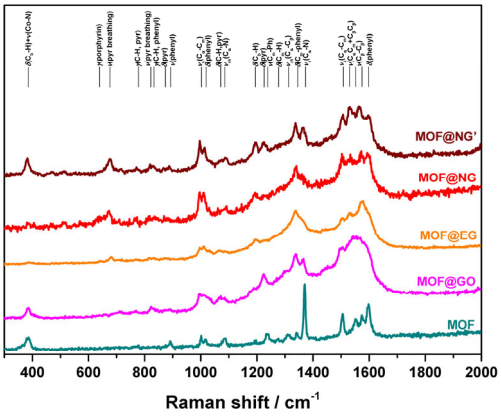

Figure S14 Raman spectra of **MOF, MOF@GO, MOF@EG, MOF@NG** and **MOF@NG'.**

Table S6 Assignment of the Raman bands of MOF-graphene catalysts [S17].

MOF	MOF@GO	MOF@EG	MOF@NG	MOF@NG'	Assignment
387.7	387.7	387.7	380.0	382.8	ν(Co-N)
(-)	(-)	639.0	636.9	639.0	γ(por)
(-)	(-)	680.6	672.8	676.7	ν(pyr breathing)
777.2	771.2	769.8	771.5	771.5	γ(C-H, pyr)
(-)	822.6	816.3	818.0	820.1	ν(pyr breathing)
(-)	837.1	832.8	836.7	832.8	γ(C-H, Ph)
874.4	873.4	874.4	870.5	867.0	δ(pyr)
892.0	889.6	876.9	883.2	887.1	ν(ph)
1002.0	995.6	995.6	995.6	997.1	ν_s(C_a-C_m)
1018.6	1007.3	1010.8	1010.8	1014.7	δ(Ph)
(-)	1072.8	1066.5	1061.5	1067.9	δ(C-H,pyr)
1085.5	1085.6	1088.0	1093.3	1090.4	ν_{as}(C_a-N)
1194.4	1190.5	1194.4	1194.4	1196.9	δ(C_b-H)
(-)	1225.8	1225.8	1225.8	1225.8	δ(pyr)
1238.5	(-)	(-)	1237.4	1237.4	ν(C_m-Ph)
1277.6	(-)	(-)	(-)	(-)	δ(C_m-H)
1311.8	1307.9	(-)	(-)	(-)	ν_{as}(C_a-C_b)
1343.8	1339.9	1338.5	1339.9	1338.5	δ(C_m-Ph)
1372.7	1366.4	1367.8	1363.9	1366.4	ν_s(C_a-N)
1508.0	1508.0	1508.0	1505.6	1508.0	ν_s(C_a-C_m)
1529.5	1529.5	1529.5	1533.4	1532.0	ν(C_aC_m+C_bC_b)
1552.1	1552.1	1553.5	1548.6	1549.6	ν(C_b-C_b)
1575.0	1575.0	1575.0	1575.0	1563.7	
1599.0	1602.8	1603.9	1595.1	1599.0	δ(Ph)

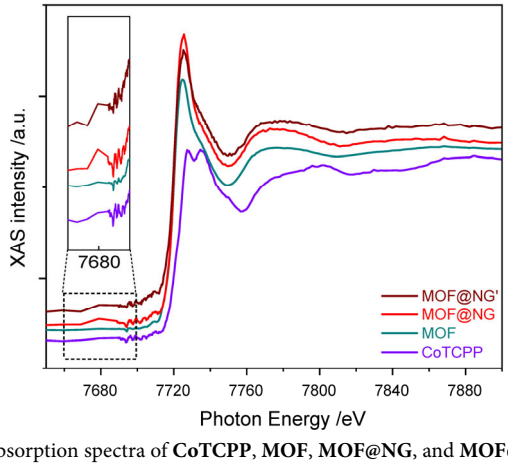

Figure S15 Cobalt *K*-edge near-edge X-ray absorption spectra of **CoTCPP**, **MOF**, **MOF@NG**, and **MOF@NG'**. The pre-edge region around 7680 eV are magnified in the inset. For **MOF@NG** and **MOF@NG'**, the pre-edge peak at 7679 eV, originated from the Co 1s→3d transition, were more intense than those of MOF and CoTCPP, indicating the alternation of the ligand field strength induced by the docking with graphene substrate [S18].

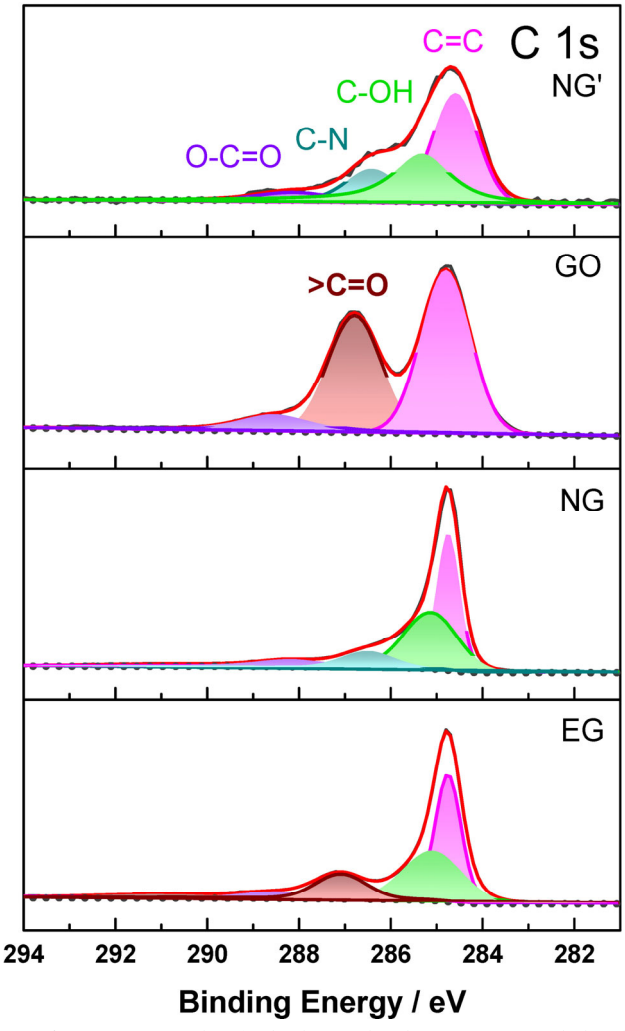

Figure S16 High resolution C *1s* spectrum of **EG**, **NG**, **GO** and **NG'**. The deconvoluted magenta, green, dark red, dark cyan and violet peaks are assigned to C=C, C-OH, C-N, >C=O and O-C=O, respectively.

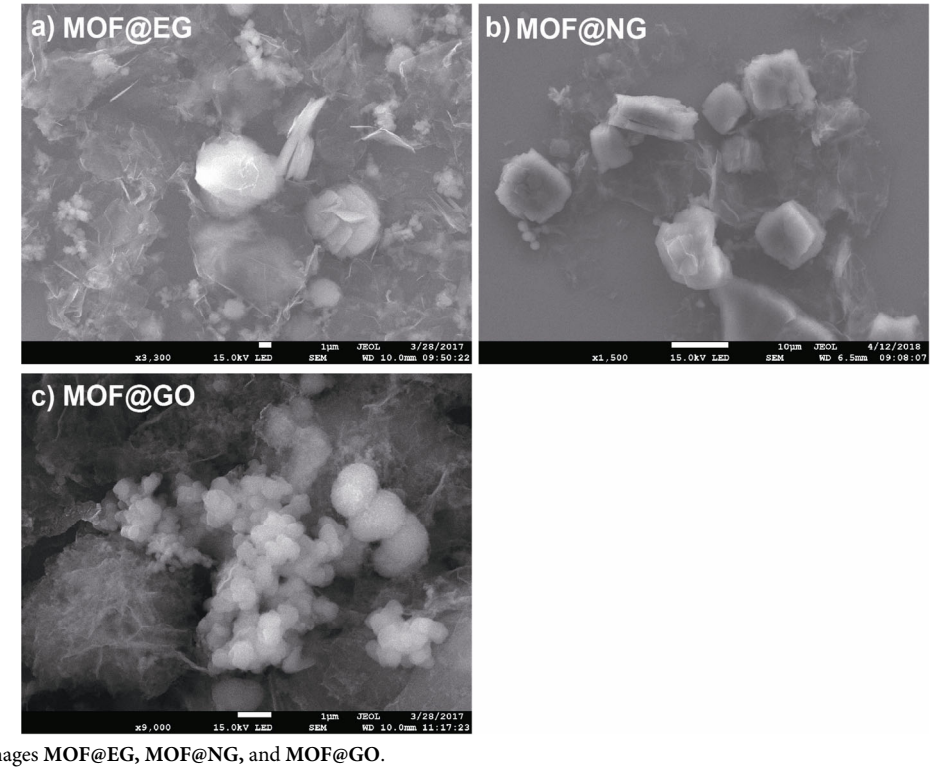

Figure S17 SEM images **MOF@EG, MOF@NG,** and **MOF@GO**.

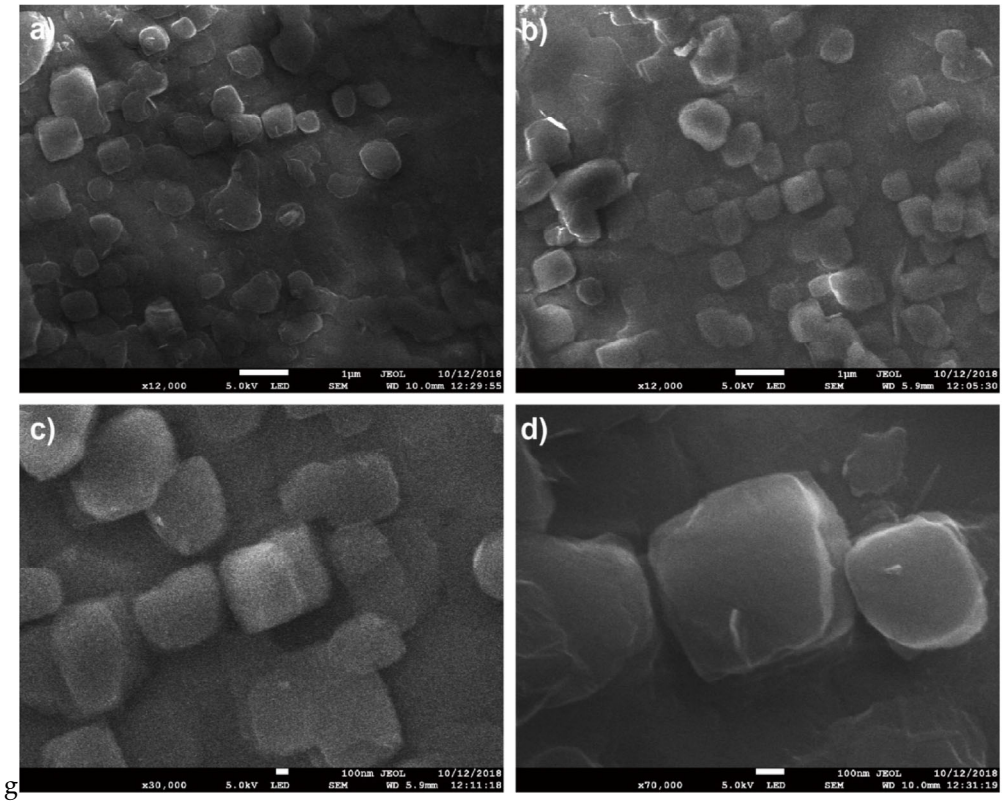

g

Figure S18 SEM images of **MOF@NG'** with different magnification.

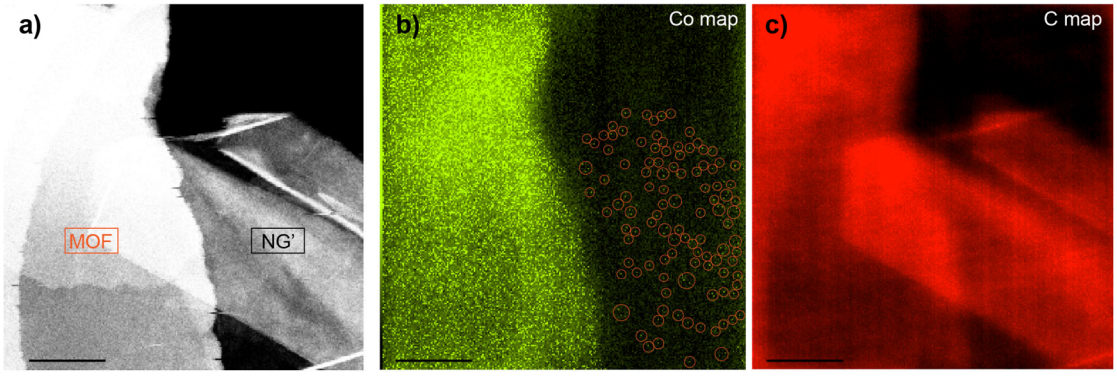

Figure S19 Electron energy loss spectroscopic (EELS) compositional map of **MOF@NG'**. Samples were crushed, sonicated and then drop-casted onto copper grid for EELS compositional map characterization on JEOL Grand-ARM 300F. a) Bright-field TEM image of **MOF@NG'** sample; b) Cobalt map of the sample in the same region. Compared with bulky MOF, the dispersed signals with size of about ~7 nm were dispersed on **NG'**. This suggests that MOFs were uniformly docked onto **NG'** substrate; c) Carbon map of the sample.

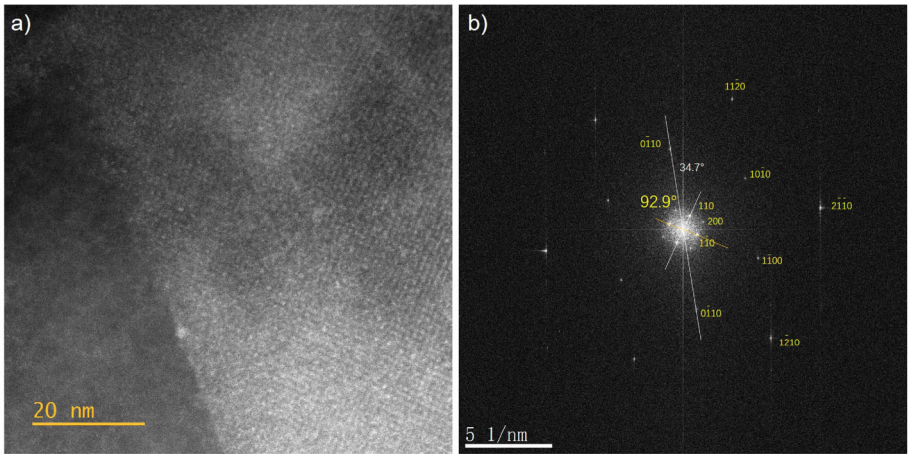

Figure S20 a) High-angle annular dark field STEM (HAADF-STEM) image of **MOF@NG'** showing tetragonal lattice of MOF; b) FFT of the whole region showing both tetragonal pattern of MOF and hexagonal pattern of nitrogen doped graphene. The intersection angle is estimated to be 34.7°.

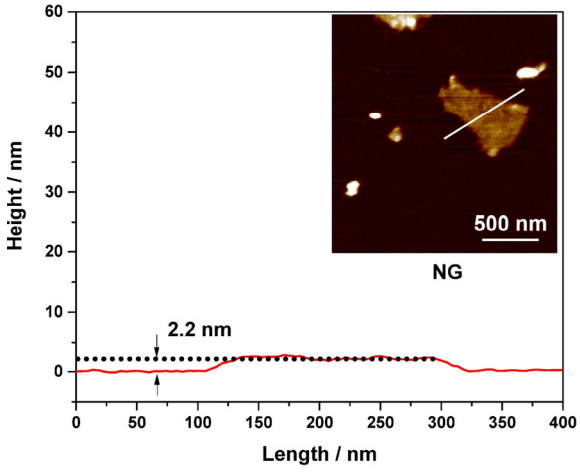

Figure S21 Atomic force microscopic image and height profile of **NG**. Such height corresponds to ~3 layers of graphene taking the dead space between Si substrate and graphene into consideration according to Ref. [S19].

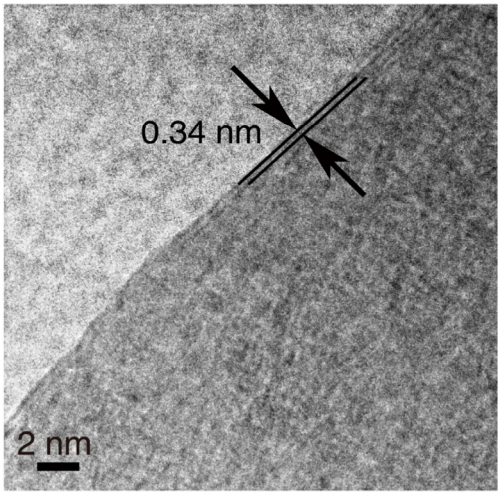

Figure S22 High resolution TEM image of NG showing 2 layers.

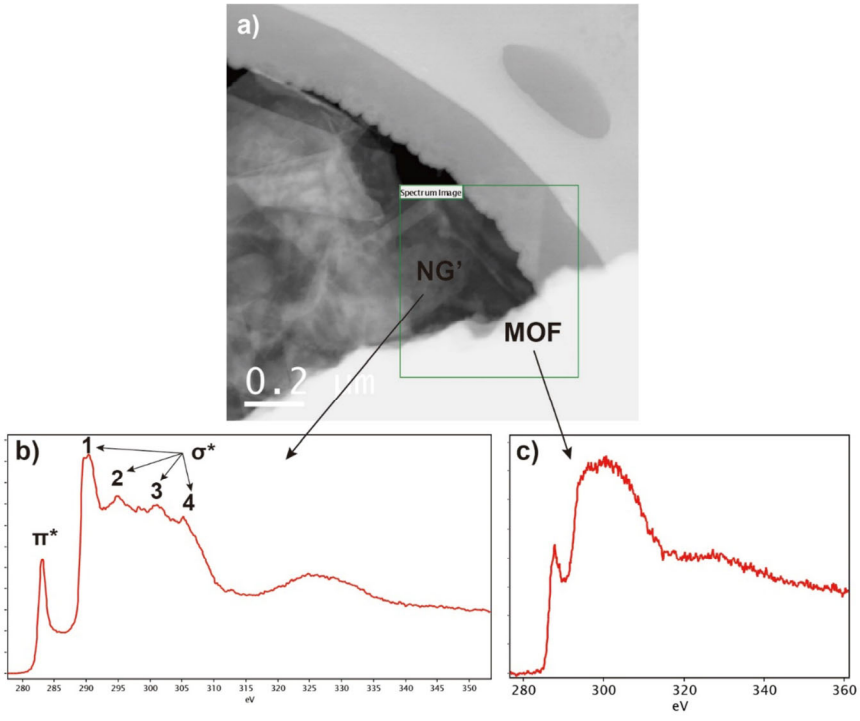

Figure S23 Electron energy-loss spectra of **MOF** and **NG'**. a) EELS captured with area containing **MOF@NG'** and **MOF**; the EELS of **NG'** and **MOF** are shown in b) and c), respectively. The EELS of **NG'** shows a distinctive 1 s to σ* transitions that splits into four peaks [peak 1 to 4 in b], indicating that carbon is sp^2 hybridized. The EELS of MOF do not have such feature, showing a broadened peak at corresponding binding energy.

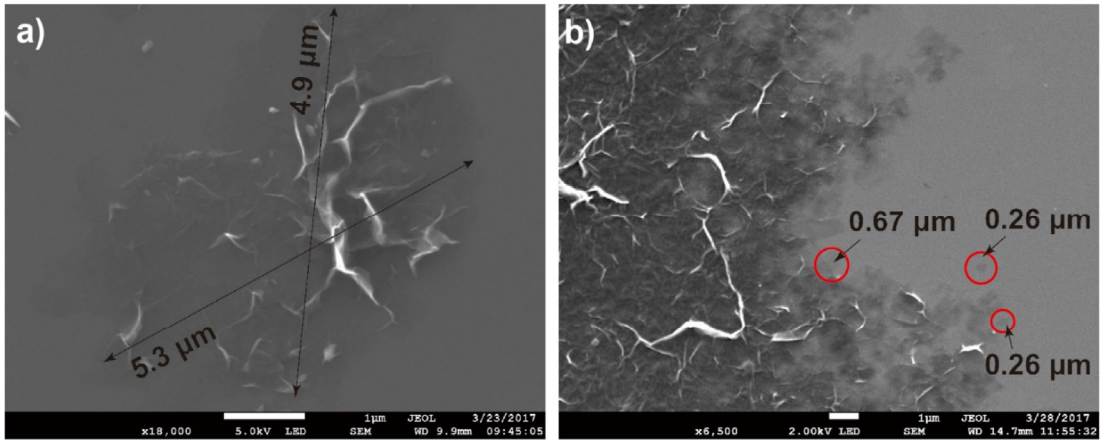

Figure S24 SEM images of a) **NG** and b) **NG'**. Red circles indicate a single sheet of **NG'**. High power sonication leads to the cleavage of large flakes of graphene to smaller one, as indicated from Ref. [S20].

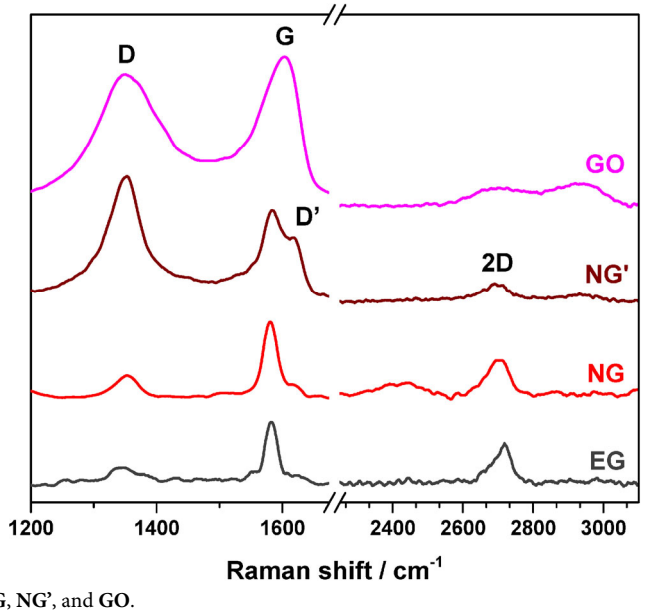

Figure S25 Raman spectra of **EG**, **NG**, **NG'**, and **GO**.

The corresponding inter-defect distance is 80.7, 68.7, 21.4, and 14.0 nm which are calculated according to the Tuinstra-Koenig equation [S21]:

$$L_a = 2.4\times10^{-10}\lambda^4\left(\frac{I_D}{I_G}\right)^{-1}$$

in which L_a the interdefect distance, λ the wavelength of the light source, I_D, I_G the intensity of D peak and G peak, respectively.

References

[S1] K. Parvez, Z.S. Wu, R.J. Li, X.J. Liu, R. Graf, X.L. Feng, K. Müllen, *J. Am. Chem. Soc.* **2014**, *136*, 6083.
[S2] E. Y. Choi, C. A. Wray, C. H. Hu and W. Choe, *CrystEngComm* **2009**, *11*, 553.
[S3] C.E. Kibbey, M.E. Meyerhoff, *Anal. Chem.* **1993**, *65*, 2189.
[S4] W. Zhang, A. U. Shaikh, E. Y. Tsui, T.M. Swager, *Chem. Mater.* **2009**, *21*, 3234.
[S5] B. Lim, M. Jiang, P. H. C. Camargo, E. C. Cho, J. Tao, X. M. Lu, Y. M. Zhu, Y. N. Xia, *Science* **2009**, *324*, 1302.
[S6] S. F. Xie, S.-I.Choi, N. Lu, L. T. Roling, J. A. Herron, L. Zhang, J. H. Park, J. G. Wang, M. J. Kim, Z. X. Xie, *Nano Lett.* **2014**, *14*, 3570.
[S7] D. L. Wang, H. L. Xin, R. Hovden, H. S. Wang, Y. C. Yu, D. A. Muller, F. J. Disalvo, H. D. Abruna, *Nat. Mater.* **2013**, *12*, 81.
[S8] J.H. Yang, J. Yang, J.Y. Ying, *ACS Nano* **2012**, *6*, 9373.
[S9] I. Hijazi, T. Bourgeteau, R. Cornut, A. Morozan, A. Filoramo, J. Leroy, V. Derycke, B. Jousselme and S. Campidelli, *J. Am. Chem. Soc.* **2014**, *136*, 6348.
[S10] P.-J. Wei, G.-Q. Yu, Y. Naruta, J.-G. Liu, *Angew. Chem. Int. Ed.* **2014**, *53*, 6659.
[S11] A. Choi, H. Jeong, S. Kim, S. Jo, S. Jeon, *Electrochim. Acta* **2008**, *53*, 2579.
[S12] Z. J. Wang, H. T. Lei, R. Cao, M. N. Zhang, *Electrochim. Acta* **2015**, *171*, 81.
[S13] S. K. Kim, S. Jeon, *Electrochem. Commun.* **2012**, *22*, 141.
[S14] M. Jahan, Q. L. Bao, K. P. Loh, *J. Am. Chem. Soc.* **2012**, *134*, 6707.

[S15] H. J. Tang, H. J. Yin, J. Y. Wang, N. L. Yang, D. Wang, Z. Y. Tang, *Angew. Chem. Int. Ed.* **2013**, 52, 5585.
[S16] A. Morozan, S. Campidelli, A. Filoramo, B. Jousselme, S. Palacin, *Carbon* **2011**, *49*, 4839.
[S17] J. M. Wan, H. Q. Wang, Z. Z. Wu, Y. C. Shun, X. M. Zheng, D. L. Phillips, *Phys. Chem. Chem. Phys.* **2011**, *13*, 10183.
[S18] R. Sarangi, J. Cho, W. Nam, E. I. Solomon, *Inorg. Chem.* **2011**, *50*, 614.
[S19] Z. G. Cheng, Q. Y. Zhou, C. X. Wang, Q. A. Li, C. Wang, Y. Fang, *Nano Lett.* **2011**, *11*, 767.
[S20] Y. Hernandez, V. Nicolosi, M. Lotya, F. M. Blighe, Z. Y. Sun, S. De, I. T. McGovern, B. Holland, M. Bryne, Y. K. Gun'ko, J. J. Boland, P. Niraj, G. Duesberg, S. Krishnamurthy, R. Goodhue, J. Hutchison, V. Scardaci, A. C. Ferrari, J. N. Coleman, *Nat. Nanotechnol.* **2008**, *3*, 563.
[S21] F. Tuinstra, J. L. Koenig, *J. Chem. Phys.* **1970**, *53*, 1126.